

# How screened exchange improves on violations of the Pauli principle in the Random Phase approximation of jellium

P. Ziesche

*Max-Planck-Institut für Physik komplexer Systeme  
Nöthnitzer Str. 38, D-01187 Dresden, Germany*

F. Hummel

*Computational Materials Physics, University Wien  
Sensengasse 8/12, A-1090 Wien, Austria*

(Dated: draft of July 20, 2022)

Within many-body perturbation theory (MBPT) of the spin-unpolarized jellium the second order exchange-term is explicitly renormalized using the Random Phase Approximation (RPA). Regarding total energies this has been studied under the name Second Order Screened Exchange (SOSEX). We study the pair correlation function (PCF) for parallel spins to investigate to what extend the exchange terms correct for violations of the Pauli principle introduced by the RPA. The PCF is directly evaluated for the thermodynamic limit by means of a Monte-Carlo integration of the imaginary frequency propagators of the homogeneous electron gas.

## I. INTRODUCTION

The uniform or homogeneous electron gas (HEG) is a prototypical model for a neutral metallic system assuming homogeneous positive background charge rather than atomic ions. Despite this simplification the HEG cannot be solved by finite order perturbation theory due to the far reaching character of the Coulomb interaction, which leads to divergences in all orders. However, one can arrive a finite and meaningful result by summing over all orders of the perturbation before summing over all states occurring in the perturbation terms — a process called renormalization. Macke [1] was the first who performed that renormalization and calculated, what was later termed Random Phase Approximation (RPA). For the HEG this recipe has been successfully applied to the total energy  $e$ , the momentum distribution  $n(k)$ , and to the structure factor  $S(q)$ . From a Fourier transform of  $S(q)$  one can obtain the

pair correlation function (PCF)  $g(r)$ , which exhibits a major deficiency of the RPA. Due to the Pauli exclusion principle the PCF of parallel electrons is expected to be zero at the electron coalescence point  $r = 0$ . In the RPA this is, however, not the case.

As pointed out by Goldstone [15] this does not come as a surprise. Diagrams do not respect the Pauli exclusion principle individually. Violations in one type of diagram are only corrected by other diagrams of the same order but of different topology where the offending states are exchanged. In finite order perturbation theory, such as Møller–Plesset theory, all diagrams of each order can be included in order to respect the Pauli principle, however, the renormalization process of the RPA disregards exchange type diagrams entirely.

The lowest order exchange diagram, shown in Fig. 2(a) is finite and does not require renormalization as found by Onsager *et al.* [7] who calculated it even analytically (!). Screening on of the two bare Coulomb interactions of the diagram in Fig. 2(a) yields finite results for all orders which were also found to be fortuitously close to quantum Monte-Carlo results [14]. So far, this class of diagrams, termed second order screened exchange correction, has only been studied for total energies. Its contribution to the structure factor from diagram in Fig. 2(c) and to what extend it improves on the violations of the Pauli principle are subject of the present paper.

All the characteristic quantities of the HEG, such as the correlation energy  $e_{\text{corr}}$ , depend on  $r_s$ , which is the radius of a sphere, containing on average just one electron. Particle number fluctuations beyond that follow from the pair-correlation functions  $g_{a,p}$  as functions of  $r$  and (parametrically) of  $r_s$  for electron pairs with antiparallel (a) and parallel (p) spins [2]. For a recent parametrization of  $e_{\text{corr}}(r_s)$  see [33]; in [17] results of MC calculations are analytically analyzed. The limiting case  $r_s = 0$  corresponds to the ideal Fermi gas. The above mentioned failure of MBPT makes the function  $e_{\text{corr}}(r_s)$  singular at  $r_s = 0$  with  $r_s^2 \ln r_s$ . A similar peculiar behavior show  $n(k)$  for  $k \rightarrow 1$  (i.e. near the Fermi surface) and  $S(q)$  for  $q \rightarrow 2$ .

Whereas the Coulomb hole  $g_a$ , with  $g_a(0) = 1 - \mathcal{O}(r_s)$ , arises only through the Coulomb repulsion, the larger Fermi hole  $g_p = \mathcal{O}(r^2)$  comes from the combined action of the (dominant) Pauli principle and the (correcting) Coulomb repulsion. Equivalent information is provided by the static structure factors (SFs)  $S_{a,p}(q)$ , which are obtained by the Fourier transforms of  $g_{a,p}(r)$  [3]. An analysis in terms of Feynman diagrams (see Appendix) shows, that  $S_a = S_d$  ( $d$  means "direct", to distinguish it from  $x$ ="exchange"), whereas  $S_p$  splits

according to  $S_p = S_p^{\text{HF}} + S_p^{\text{cum}}$  into a Hartree-Fock (HF) like part  $S_p^{\text{HF}}$  reducible to the correlated  $n(k)$  and a cumulant non-reducible remainder  $S_p^{\text{cum}}$  [3], which again splits according to  $S_p^{\text{cum}} = S_d - S_x$  into the direct part  $S_d$  and the corresponding exchange part  $S_x$ . Thus for  $S = S_a + S_p$  it is  $S = S_p^{\text{HF}} + 2S_d - S_x$ . These splittings have been derived in [4, 5] from the 2-body reduced density matrix and its linked-diagram representations. The same splitting follows automatically from the linked-diagrams of  $e_{\text{corr}}$  and the generalized Hellmann-Feynman theorem, see Eqs. 4 and 5. Note that the approximations for "HF" and "cum" have to base on the same footing.

At the level of the RPA the  $e_{\text{corr}}$  of the HEG has been studied [1, 6], [7]. It was extended to the static quantities  $n(k)$  [8, 9],  $S(q)$  [10–13], the 2-body reduced density matrix [4, 5], and also to the dynamic quantities  $G(k, \omega), S(k, \omega)$  with plasmon frequency and plasmon damping [34, 35]. This paper continues [4, 5] and explains the partitioning of  $S_p$  which includes the Pauli principle and shows that RPA neglects important contributions to the spin-parallel part of the structure factor as well as to second order of  $n(k)$ , stemming from exchange effects.

### Remark on the notation

The momenta  $k = |\mathbf{k}|$  and  $q = |\mathbf{q}|$  are measured in units of  $k_F = 1/(\alpha r_s)$ , energies in  $k_F^2$ ,  $t(\mathbf{k}) = \mathbf{k}^2/2$ ,  $v(\mathbf{q}) = q_c^2/q^2$ ,  $q_c^2 = 4\alpha r_s/\pi$ ,  $\alpha = (4/9\pi)^{1/3}$ ,  $\omega_{\text{pl}}^2 = q_c^2/3$ ,  $a = (1 - \ln 2)/\pi^2 = 0.0311$  is referred to as Macke number, and  $x = (\alpha r_s)^2 \ln r_s$ . There are several functions of  $q$ , often the argument is not given explicitly for convenience, e.g.  $S$  means  $S(q)$ , respectively  $S(q, r_s)$ . What is in [4] named  $(1/2)F(q)$ , is here and in [5] denoted by  $F(q)$ .

## II. THE PAIR CORRELATION FUNCTION AND THE STRUCTURE FACTORS

As already mentioned above, the SF  $S$  splits according to  $S = S_a + S_p$  into a spin-antiparallel and a spin-parallel part  $S_{a,p}$ . The same holds for the pair densities  $g_{a,p}$ . The SFs  $S_{a,p}$  are normalized according to

$$\int_0^\infty d(q^3) (-)S_a(q) = [1 - g_a(0)], \quad \int_0^\infty d(q^3) [1 - S_p(q)] = 1, \quad (1)$$

and they contribute to the total interaction energy  $v = v_a + v_p$  with

$$v_a = \frac{3\omega_{\text{pl}}^2}{4} \int_0^\infty dq S_a(q), \quad v_p = -\frac{3\omega_{\text{pl}}^2}{4} \int_0^\infty dq [1 - S_p(q)] \quad \curvearrowright \quad v = -\frac{3\omega_{\text{pl}}^2}{4} \int_0^\infty dq [1 - S(q)] \quad (2)$$

as functions of  $r_s$ . The energy in lowest order is  $v_1 = -(3\omega_{\text{pl}}/4)$ . From the SFs  $S_{a,p}$  follow the parallel-spin pair-correlation functions (PCFs)

$$g_a(r) = 1 + \int_0^\infty d(q^3) \frac{\sin qr}{qr} S_a(q), \quad g_p(r) = 1 - \int_0^\infty d(q^3) \frac{\sin qr}{qr} [1 - S_p(q)] \quad (3)$$

with  $g_p(0) = g'_p(0) = 0$  for the Pauli principle, which makes the parallel-spin PCF to start with  $g_p(r) = (1/2)g''_p(0)r^2 + \dots$ . The conservation of particles implies  $S_{a,p}(0) = 0$ . This makes also

$$\alpha^3 \int_0^\infty d(r^3) [1 - g_p](r) = 1, \quad \int_0^\infty d(r^3) [1 - g_a](r) = 0,$$

known as the perfect screening SR (or charge neutrality condition). Important correlation parameters are  $g_a(0)$  and  $g''_p(0)$ . As already Goldstone mentioned, it may be violated with  $g_p(0) \neq 0$ , if not all exchange processes are included. The small- $q$  limit  $S(q \rightarrow 0) = q^2/(2\omega_{\text{pl}}) + \dots$  is the plasmon SR, see refs. in [17]. Using  $S_{a,p}$  of Eqs. (15) and (18) yields results for  $g_{a,p}$ , which qualitatively agree with Fig. 5 of [18].

The energy  $e$  is a sum of topologically distinct vacuum diagrams, each of them built up from the 1-body propagator  $G_0(\mathbf{k}, \omega)$ , which contains  $t(\mathbf{k}) = \mathbf{k}^2/2$ , and from the static (frequency independent) Coulomb repulsion  $v(\mathbf{q}) = q_c^2/\mathbf{q}^2$ . The p-h-lines form closed loops, linked by interaction lines. Each interaction line comes from a p-h-line and runs into another or the same p-h-line (forming thus vertices). Each closed loop appears twice according to the two spin orientations. Each vacuum diagram consists of closed loops linked by interaction lines defining thus a functional of  $t(\mathbf{k})$  and  $v(\mathbf{q})$ . Then  $n(k)$  and  $S(q)$  follow from the generalized Hellmann-Feynman theorem:

$$n(k) = \frac{\delta e}{\delta t(\mathbf{k})}, \quad t = \int_0^\infty d(k^3) n(k) \frac{k^2}{2}, \quad \int_0^\infty d(k^3) n(k) = 1, \quad (4)$$

$$S(q) = 1 + 16\pi \frac{\delta e}{\delta v(\mathbf{q})}, \quad v = -\frac{3\omega_{\text{pl}}^2}{4} \int_0^\infty dq [1 - S(q)], \quad \int_0^\infty d(q^3) [1 - S(q)] = 2[1 - g(0)]. \quad (5)$$

In Eq. (5) the differential operator cuts out successively interaction lines according to the product rule. In Eq. (4) p-h-lines are successively cut.

It is easy to show by means of Eq. (5) that the vacuum diagrams of  $e$  are transformed quite automatically to the 2-point diagrams of  $S_{d,x}$  and  $F$  as

$$S_a = S_d, \quad S_p = [1 - F] + [S_d - S_x] = S_p^{\text{HF}} + S_p^{\text{cum}}, \quad (6)$$

where the 'direct' diagrams  $S_d$  are linking **two** closed loops. The exchange diagrams  $S_x$  are as in Fig. 2(a), where the cutting procedure happens only at **one** and the same closed loop. In the term of Fig. 2(c) are such 2-point  $S_p$ -diagrams addressed, which have no links between its left and right half. Such  $S_p$ -diagrams can be summed up according to  $G_0 \rightarrow G$ , see Fig. III, to give the HF-function  $F$  (with  $n(k) =$  correlated momentum distribution [4, 5, 8, 9, 21–24])

$$F(q) = \int \frac{d^3 k}{4\pi/3} n(k) n(|\mathbf{k} + \mathbf{q}|). \quad (7)$$

The HF-function exhibits the following properties

$$\int \frac{d^3 q}{4\pi/3} F(q) = 1, \quad F(q \rightarrow \infty) \sim 1/q^8, \quad (8)$$

where  $F(0)$  is referred to as Löwdin number. Its lowest order expansion is

$$F_0(q) = \left[ 1 - \frac{3q}{4} + \frac{q^3}{16} \right] \Theta(2 - q), \quad (9)$$

and its Fourier transform follows from the 1-matrix in  $r$ -representation

$$f(r) = \int_0^\infty d(k^3) \frac{\sin kr}{kr} n(k) \Rightarrow \int_0^\infty d(q^3) \frac{\sin qr}{qr} F(q) = [f(r)]^2. \quad (10)$$

This shows, that  $S_p$  splits quite naturally into a reducible HF-part  $S_p^{\text{HF}} = 1 - F$  [which needs the knowledge of the correlated  $n(k)$ ] and a non-reducible cumulant remainder  $S_p^{\text{cum}} = S_d - S_x$  as in Eq. (6) in agreement with the linked-diagram theorem [25]:  $S_{d,x}$  are sums of linked diagrams, the unlinked ones are in the HF term. In addition to the norms (1), (3) and (7), it holds

$$\int_0^\infty d(q^3) [S_d - S_x](q) = 0, \quad \int_0^\infty dqq^4 [S_d - S_x](q) = \frac{3}{4}t - g_p''(0)$$

The analogous splitting of the PCF is  $g_p = g_p^{\text{HF}} + g_p^{\text{cum}}$  with

$$g_p^{\text{HF}}(r) = 1 - [f(r)]^2, \quad g_p^{\text{cum}}(r) = \int_0^\infty d(q^3) \frac{\sin qr}{qr} [S_d - S_x](q). \quad (11)$$

Similarly, the splitting of the interaction energy is  $v_p = v_p^{\text{HF}} + v_p^{\text{cum}}$  with

$$v_p^{\text{HF}} = -\frac{\omega_{\text{pl}}^2}{4} \int_0^\infty d(k^3) \int_0^\infty d(k'^3) \frac{n(k)n(k')}{|\mathbf{k} - \mathbf{k}'|^2}, \quad v_p^{\text{cum}} = \frac{3\omega_{\text{pl}}^2}{4} \int_0^\infty dq [S_d - S_x](q) \quad (12)$$

with  $v_p^{\text{HF}} \rightarrow v_1 = -(3\omega_{\text{pl}}/4)^2$  for  $r_s \rightarrow 0$ , being HF in lowest order. [The index "1" means  $v_1 \sim r_s$ .] This analysis of Eqs. (1)-(12) is in agreement with the access through the 2-body reduced density matrix [4, 5]. By the way, this reconfirms vice versa the generalized Hellmann-Feynman theorem.

The asymptotics for  $q \rightarrow \infty$  is in first order (Kimbball trick [10])

$$S_d = -\left(\frac{g_a(0)}{q^4} + \frac{g_p''(0)}{q^6} + \dots\right) \omega_{\text{pl}}^2 + \dots, \quad S_x = -\left(\frac{g_a(0)}{q^4} + \frac{4g_p''(0)}{q^6} + \dots\right) \omega_{\text{pl}}^2 + \dots. \quad (13)$$

With Eq. (6) it is  $S_a = S_d$  and  $S_p = 1 + [S_d - S_x] + \dots$  or  $S_p = 1 + (3g_p''(0)/q^6) \omega_{\text{pl}}^2 + \dots$ , see [12]. So  $S_p(q \rightarrow \infty)$  starts with a  $1/q^6$ -term, while the total SF  $S = S_a + S_p$  starts with a  $1/q^4$ -term, approaching zero from below. The quantities  $1 - g_a(0) = 0.7317 r_s + \dots$  [11] and  $2/5 - g_p''(0) = 0.2291 r_s + \dots$  [13] are correlation measures, vanishing for  $r_s \rightarrow 0$  and increasing with  $r_s$ . For  $r_s \rightarrow 0$  the correlation induced cumulant parts vanish and it remains (the uncorrelated) HF in lowest order:

$$S_p^{\text{HF}} \rightarrow S_0(q) = \left(\frac{3q}{4} - \frac{q^3}{16}\right) \Theta(2-q) + \Theta(q-2), \quad g_p^{\text{HF}} \rightarrow g_0(r) = 1 - \left(\frac{3(-r \cos r + \sin r)}{r^3}\right)^2. \quad (14)$$

The cusp singularities  $S_0(q \rightarrow 0) \sim q$  and  $\sim q^3$  make the non-oscillatory asymptotic terms of  $g_0(r \rightarrow \infty) \sim 1/r^4$  and  $\sim 1/r^6$  [26]. With Eqs. (1), (6), and (8) the cumulant term contributes to the structure factor normalization.

To gain information from the above Eqs. (1)-(14) the SFs  $F, S_{d,x}$  need to be known at least approximately. For  $S_{d,x}$  this is done within the RPA.

### A. Antiparallel-spin pairs: Coulomb hole in RPA

Fig. 1(c) shows the contribution to  $S_a$  in the lowest order of RPA:

$$S_{\text{ar}}(q) = -\frac{(3\omega_{\text{pl}})^2}{4\pi} 2q \int_0^\infty du \frac{R^2(q, u)}{q^2 + q_c^2 R(q, u)}, \quad S_a = S_{\text{ar}} + \dots. \quad (15)$$

The negative part of Fig. 5 shows  $S_a$  in RPA as a function of  $q$  and  $r_s$ . The index r denotes the RPA and the dots mean terms beyond RPA. Asymptotic properties: It has the small- $q$  asymptotics

$$S_a(q \rightarrow 0) = -\frac{1}{2} \cdot S_0(q) + \frac{1}{2} \cdot \frac{q^2}{2 \omega_{\text{pl}}} + \left[ d_4 \left( \frac{q}{\omega_{\text{pl}}} \right)^4 + d_5 \left( \frac{q}{\omega_{\text{pl}}} \right)^5 + \dots \right] \omega_{\text{pl}} + \dots \quad (16)$$

with the  $r_s$ -independent linear-cubic or ideal-gas term  $S_0$  of Eq. (14) and with a plasmon term  $\sim q^2$  (more precisely one half of it, the other half comes from  $S_p$ ). The  $r_s$ -dependent coefficients are in agreement with the bounds estimated by Iwamoto [27]. For  $r_s \approx 5$  it is  $d_4 \approx -0.0748$  and  $d_5 \approx +0.024$ .  $S_a(0) = 0$  corresponds to the perfect screening SR.  $S_a$  of Eq. (15) has the large- $q$  asymptotics  $\sim -(1/q^4 + 0.4/q^6 + \dots)$  as  $S_x$ . But cusp and curvature theorems demand a decoration by correlation parameters according to Eq. (13).

Integral properties:  $S_a$  determines the antiparallel-spin pair-correlation function  $g_a$ , in particular the norm of  $S_a = S_d$  fixes the near-field correlation parameter  $g_a(0)$  in RPA [according to Eq. (1), respectively Eq. (3) for  $r = 0$ ].  $S_{\text{ar}}$  of Eq. (15) in the interaction energy  $v_a$  of Eq. (2) gives

$$v_{\text{ar}} = -\frac{1}{2} \cdot \frac{27 \omega_{\text{pl}}^4}{8\pi} \int_0^\infty du \int_0^\infty d(q^2) \frac{R^2(q, u)}{q^2 + q_c^2 R(q, u)}. \quad (17)$$

For  $r_s \rightarrow 0$ , this behaves as  $v_a \rightarrow a \cdot x + \dots$  [with  $a = (1 - \ln 2)/\pi^2$  and  $x = (\alpha r_s)^2 \ln r_s$ ].

## B. Parallel-spin pairs: Fermi hole beyond RPA

The exchange term  $S_x$  is part of the Fermi hole  $S_p$ , as seen from Eq. (6). The formula corresponding to Fig. 2(c) yields after a tedious derivation with contour integrations (P.Z.):

$$S_{\text{xr}}(q) = -3 \int \frac{d^3 k_1 d^3 k_2}{(4\pi)^2} \int_{-\infty}^{+\infty} \frac{k}{2\pi} \frac{du}{(k^2 u^2 + \varepsilon_1^2)(k^2 u^2 + \varepsilon_2^2)} \cdot \frac{q_c^2}{k^2 + q_c^2 R(k, u)}, \quad (18)$$

with  $k_{1,2} < 1 < |\mathbf{k}_{1,2} + \mathbf{q}|$ ,  $\mathbf{k} = \mathbf{k}_1 + \mathbf{k}_2 + \mathbf{q}$ ,  $\varepsilon_1 = t(\mathbf{k}_2 + \mathbf{q}) - t(\mathbf{k}_1)$ ,  $\varepsilon_2 = t(\mathbf{k}_1 + \mathbf{q}) - t(\mathbf{k}_2)$ , and  $t(\mathbf{k}) = \mathbf{k}^2/2$ . One way to check this complicated integral is, to remove the screening term  $R(q, u)$  in the denominator. This yields the well-known energy denominator for the exchange term in lowest order,

$$S_{\text{x1}}(q) = -\frac{\omega_{\text{pl}}^2}{(4\pi/3)^2} \int \frac{d^3 k_1 d^3 k_2}{\mathbf{q} \cdot (\mathbf{k}_1 + \mathbf{k}_2 + \mathbf{q})} \frac{1}{(\mathbf{k}_1 + \mathbf{k}_2 + \mathbf{q})^2} \quad (19)$$

with  $k_{1,2} < 1 < |\mathbf{k}_{1,2} + \mathbf{q}|$ , as it should. Note that the  $u$ -integral over  $\varepsilon_1 \varepsilon_2$  in the denominator yields the same as over  $(k^2 u^2 + \varepsilon_1 \varepsilon_2)$ . This result strengthens the confidence in the correctness of Eq. (18). The exchange integral (19) has been calculated by Gutlé and Cioslowski [5, 28]. From (19) follows

$$S_{x1}(q \rightarrow 0) = -\frac{3}{4\pi}(2 \ln 2 - 1) r_s q + \dots$$

With  $S_x$  also  $g_p^{\text{cum}}$  and  $v_p^{\text{cum}}$  are available, see Eqs. (11) and (12).

Unfortunately the integral (18) is not known so far as an explicit function of  $q$  and  $r_s$ . It can, however, be evaluated numerically by means of a MC integration. To this purpose we change from the frequency integrations  $\int d\omega_i$  [S-matrix theory after Feynman, shortly described before Eq. (4)] to the equivalent time-ordered integrations  $\int dt_i$  [Goldstone treatment]. We first draw uniformly distributed momenta  $\mathbf{k}_1$  and  $\mathbf{k}_2$  such that  $|\mathbf{k}_{1,2}| < 1 < |\mathbf{k}_{1,2} + \mathbf{q}|$ . Subsequently, we integrate over  $u$  for each sampled pair  $\mathbf{k}_{1,2}$  with a weighted Gauss-Kronrod rule using the term  $(k^2 u^2 + \varepsilon_1 \varepsilon_2) / ((k^2 u^2 + \varepsilon_1^2)(k^2 u^2 + \varepsilon_2^2))$  as the weighting function since it can be integrated analytically. For each value of  $q$  we find 15 and 100000 samples sufficient for the frequency integration and momentum integration, respectively. Fig. 5 shows the exchange structure factor as a function of  $q$  for different values of  $r_s$ . The error bars give the 95% confidence interval estimated from the variance of the integrand. The statistical uncertainty of the variance is in turn estimated using the fourth central statistical moment.

The results for  $S_x$  vs.  $q$  are shown in Fig. 5. The  $S_x$  of Eq. (18) violates the large- $q$  behavior by showing 1 and 2/5 instead of the correlation parameters  $g_a(0)$  and  $g_p''(0)$ , respectively. For  $S_p$  with Eqs. (6) and (13) it holds for  $q \rightarrow \infty$

$$S_p = 1 + \left( \frac{3g_p''(0)}{q^6} + \dots \right) \omega_{\text{pl}}^2 + \dots \Rightarrow S = 1 - \left( \frac{g_a(0)}{q^4} - \frac{2g_p''(0)}{q^6} + \dots \right) \omega_{\text{pl}}^2 + \dots, \quad (20)$$

where the on-top-Fermi-hole curvature  $g_p''(0)$  comes from

$$g_p''(0) = \frac{4}{3}t - \int_0^\infty dq q^4 [S_d - S_x](q), \quad \int_0^\infty d(q^3) [S_d - S_x](q) = 0, \quad (21)$$

see Appendix A in [5]. Eq. (21) shows, how exchange influences both  $S_p$  and  $n(k)$  via  $t$  and how this is mutually coupled.  $S_{d,x}$  approach zero from below. (21) holds, assuming all exchange diagrams are included, which is not the case for RPA.

According to [1, 16] the high-density limits in lowest order of RPA

$$e = t_0 + v_1 + a \cdot x + \dots \quad \text{and} \quad v = v_1 + 2a \cdot x + \dots \quad (22)$$

hold [with  $a = (1 - \ln 2)/\pi^2$  and the shorthand  $x = (\alpha r_s)^2 \ln r_s$ ]. On the other hand it is  $v = v_a + v_p$  with Eqs. (2) and (17) and  $v_a = a \cdot x + \dots$ . This lets one expect  $v_p \rightarrow v_1 + a \cdot x + \dots$  for  $r_s \rightarrow 0$ .

The violation of the Pauli principle shows the need to search for further diagrams, which revoke the deficiency. It remains to study whether and how the plasmon sum rule follows from (15) and (18).

### III. SUMMARY

For the pair-correlation function or structure factor (SF) one has to distinguish electron pairs with antiparallel (a) and and parallel (p) spins. The spin-antiparallel SF  $S_a$  is within RPA well-known. The spin-parallel SF  $S_p$  proves to be a sum of a reducible HF-like term  $S_p^{\text{HF}}$  and a non-reducible cumulant remainder  $S_p^{\text{cum}}$ . This  $S_p^{\text{cum}}$  contains (besides  $S_a = S_d$ ) an exchange term  $S_x$ , which is calculated here for the first time numerically.

If  $n(k)$  is available, then  $t$  and  $S_p^{\text{HF}} = S_0 + \dots$  can be calculated with  $v_p^{\text{HF}} = v_1 + \dots$  and  $g_p^{\text{HF}} = g_0 + \dots$ . If  $S_d$  is available, then  $v_a$  and  $g_a$  in particular  $g_a(0)$  can be calculated. If  $S_x$  is available, then  $S_p^{\text{cum}} = S_d - S_x$ ,  $g_p^{\text{cum}}$ ,  $g_p = g_p^{\text{HF}} + g_p^{\text{cum}}$ , in particular  $g_p''(0)$ , and  $v_p^{\text{cum}}$ ,  $v_p = v_p^{\text{HF}} + v_p^{\text{cum}}$ ,  $v = v_a + v_p$  and  $e = t + v$  and  $e_{\text{corr}} = e - t_0 - v_1$  can be calculated, hopefully obeying the Lieb-Oxford bound  $e_{\text{corr}} \geq B v_1$  with  $B = 1, \dots, 1.93$  for  $r_s = 0, \dots, \infty$  [29, 30] and refs. therein. When going through these steps, MC results for  $S_{a,p}$  [31] should be incorporated similar as in [17]. Whereas the singular behavior of  $n(k)$  for  $k \rightarrow 1^\pm$  is known (in RPA), the special behavior of  $S_{d,x}(q)$  for  $q \rightarrow 2^\pm$  [curvature jump, responsible for the  $r_s$ -dependent Friedel oscillations of  $g_{a,p}(r)$ ] is not known so far.

Quite another question is, how the analysis presented here applies to recent attempts to split the Coulomb electron-electron repulsion into a short-range and a long-range part, see [32] and to use different approximations for these long- and short-range contributions to the exchange and correlation energy.

### Acknowledgment

The authors acknowledge P. Fulde and the Max Planck Institute for the Physics of Complex Systems Dresden for supporting this work and we thank the  $\Psi_{\mathbf{k}}$  community for helping to build fruitful cooperation as well as the DPG for their exciting Spring Meetings Dresden 2014 and Berlin 2015. Thanks also to J. Cioslowski, P. Gori-Giorgi, J.P. Perdew, and A. Savin for stimulating discussions.

### Appendix: Par force course of MBPT

MBPT theory shows, that the GS energy (per particle) is given by linked Feynman diagrams of closed p-h-lines linked with each other by Coulomb interaction lines. The building elements of these vacuum diagrams are pieces of p-h-lines  $G_0(k, \omega)$  containing  $t(\mathbf{k}) = k^2/2$  [with  $k$  in units of  $k_F$  and energies in units of  $k_F^2$ ] and wavy interaction lines  $v(\mathbf{q}) = q_c^2/q^2$ . The number of interaction lines give the order of the  $e$ -diagram under consideration. Each line carries a momentum. At a vertex, where an interaction line meets a p-h-line, the momentum is conserved. The quantum kinematics - hidden in the momentum distribution  $n(k)$  and the structure factor  $S(q)$  - arise from the (generalized) Hellmann-Feynman theorems. For  $n(\mathbf{k})$  the Eq.(4) yields the well-known Migdal-formula  $n(k) = \int d\omega/2\pi i G(k, \omega)$ . The quantities  $n(k)$  and  $S(q)$  can be considered as 2 different "projections" of the vacuum diagram under consideration. In (4) a p-h-line is cut (producing thus a non-vacuum-diagram), in (5) an interaction line is cut out (producing thus in another way also a non-vacuum-diagram). The functional derivatives act on the vacuum diagrams like scissors, cutting p-h-lines or cutting out interaction lines. For such functional derivatives see App. A [20]. A theorem related to (5) is the virial theorem  $v = r_s de/r_s$  [16]. But note that the approximations for  $e, t, v$  have to base on the same footing.

---

[1] W. Macke, Z. Naturforsch. A **5**, 192 (1950). Another approach with the same result is due to D. Bohm and D. Pines (1953).

[2] P. Ziesche, J. Tao, M. Seidl, and J.P. Perdew, Int. J. Quantum Chem. **77**, 819 (2000).

[3] For the history of the cumulant concept in Statistical Physics and Many-Body theory see e.g. P. Ziesche and refs. therein in J. Cioslowski (Ed.), Many-Electron Densities and Density Matrices, p. 34, Kluwer/Plenum, New York (2000). A survey on RDMs in quantum chemistry and their cumulant representation is in W. Kutzelnigg and D. Mukherjee, *Int. J. Quantum Chem.* **110**, 2800 (1999) and in K. Kladko and P. Fulde, *Int. J. Quantum Chem.* **66**, 377 (1998). A novel interpretation of RDMs and their cumulants is in L. Kong and E.F. Valeev, *J. Chem. Phys.* **134**, 214109 (2011). see also G. H. Booth *et al.*, *Nature* **493**, 365 (2013).

[4] P. Ziesche, *Phys. Rev. A* **86**, 012508 (2012); *A* **89**, 059902(E)(2014).

[5] P. Ziesche and J. Cioslowski, *J. Modern Phys.* **5**, 725 (2014). - The paragraph with Eq. (4.11) proves to be omitted.

[6] M. Gell-Mann and K. Brueckner, *Phys. Rev.* **106**, 364 (1957).

[7] L. Onsager, L. Mittag, and M. J. Stephen, *Ann. Physik (Leipzig)* **18**, 71 (1966).

[8] E. Daniel and S.H. Vosko, *Phys. Rev.* **120**, 2041 (1961).

[9] I.O. Kulik, *Zh. Éksp. Teor. Fiz.* **40**, 1343 (1961) [Sov. Phys. JETP **13**, 946 (1961)].

[10] J.C. Kimball, *Phys. Rev. A* **7**, 1648 (1973).

[11] J.C. Kimball, *Phys. Rev. B* **14**, 2371 (1976).

[12] A.K. Rajagopal, J.C. Kimball, M. Banerjee, *Phys. Rev. B* **18**, 2339 (1978).

[13] V.A. Rassolow, J.A. Pople, and M.A. Ratner, *Phys. Rev. B* **59**, 2232 (2000).

[14] D. Freeman, *Phys. Rev. B* **15**, 5512 (1977).

[15] J. Goldstone, *Proc. Roy. Soc. A* **239**.1217, pp. 267-279. (1957)

[16] N.H. March, *Phys. Rev.* **110**, 604 (1958). For  $e(r_s)$  see e.g. H. Cong, *phys. stat. sol. (b)*, **205**, 543 (1998).

[17] P. Gori-Giorgi, F. Sacchetti, G.B. Bachelet, *Physica A* **280**, 199 (2000); *Phys. Rev. B* **61**, 7353 (2000); *Phys. Rev. B* **66**, 159901(E)(2002).

[18] P. Ziesche, *Int. J. Quantum Chem.* **90**, 342 (2002).

[19] P. Güttinger, *Z. Phys.* **73**, 169 (1932).

[20] P. Ziesche, *Ann. Physik (Berlin)* **522**, 739 (2010).

[21] P. Gori-Giorgi and P. Ziesche, *Phys. Rev. B* **66**, 235116 (2002).

[22] V. Olevano *et al.*, *Phys. Rev.B* **86**, 195123 (2012).

[23] M. Holzmann *et al.*, *Phys. Rev. Lett.* **107**, 110402 (2011).

[24] S. Huotari *et al.*, *Phys.Rev.Lett.* **105**, 086403 (2010).

- [25] P. Ziesche, *Commun. Math. Phys.* **5**, 191 (1967).
- [26] P. Ziesche, *phys. stat. sol. (b)* **242**, 2051 (2005).
- [27] N. Iwamoto, *Phys. Rev. A* **33**, 1940 (1986), Eq. (4.2)
- [28] C. Gutlé, *Comp. Phys. Commun.* **174**, 836 (2006). The marked simplification for  $q \geq 2$  is due to J. Cioslowski [5].
- [29] E.H. Lieb and S. Oxford, *Int. J. Quantum Chem.* **19**, 427 (1981).
- [30] J.P. Perdew *et al.*, *J. Chem. Phys.* **140**, 18A533 (2014).
- [31] D.M. Ceperley, *Phys. Rev. B* **18**, 3126 (1978); D.M. Ceperley and B.J. Alder, *Phys. Rev. Lett.* **45**, 566 (1980).
- [32] P. Gori-Giorgi and A. Savin, *Phys. Rev. A* **73**, 032506 (2006), A. Savin, *Chem. Phys.* **356**, 91 (2009).
- [33] T. Chachiyo, *J. Chem. Phys.* **145**, 021101 (2016) and V.V. Karasiev, *J. Chem. Phys.* **145**, 157101 (2016).
- [34] P.K. Aravind, A. Holas, and K.S. Singwi, *Phys. Rev. B* **25**, 561 (1982).
- [35] F. Brosens, J.T. Devreese, and L.F. Lemmens, *Phys. Rev. B* **21**, 1363 (1980); J.E. Alvarellos and F. Flores, *J. Phys. F: Met. Phys.* **15**, 1929 (1985); B. Holm and U. von Barth, *Phys. Rev. B* **57**, 2108 (1998).
- [36] P. Fulde, *Nature Physics* **12**, 106 (2016); see also [37].
- [37] G. Booth *et al.*, *Nature* **493**, 365 (2013).
- [38] F. Hummel *et al.*, to be published.

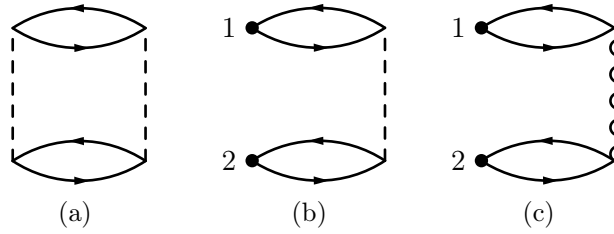


FIG. 1: (a) Divergent direct vacuum diagram of second order. (b) Divergent structure factor diagram with left interaction line cut out. (c) Convergent structure factor diagram with RPA screened right interaction line.

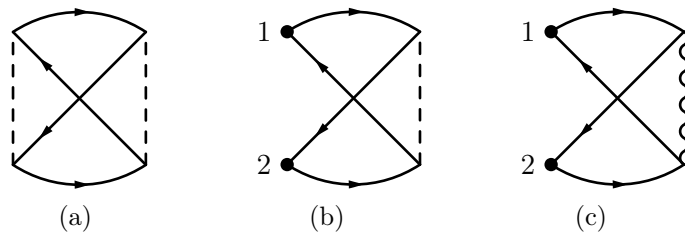


FIG. 2: (a) Convergent exchange vacuum diagram of second order corresponding to the direct diagrams of Fig. 1(a). (b) Divergent structure factor diagram with left interaction line cut out. (c) Convergent structure factor diagram with RPA screened right interaction line.



FIG. 3: In this term there are no links between the left and the right half. They can be summed up to give the HF-function  $F(q)$ .

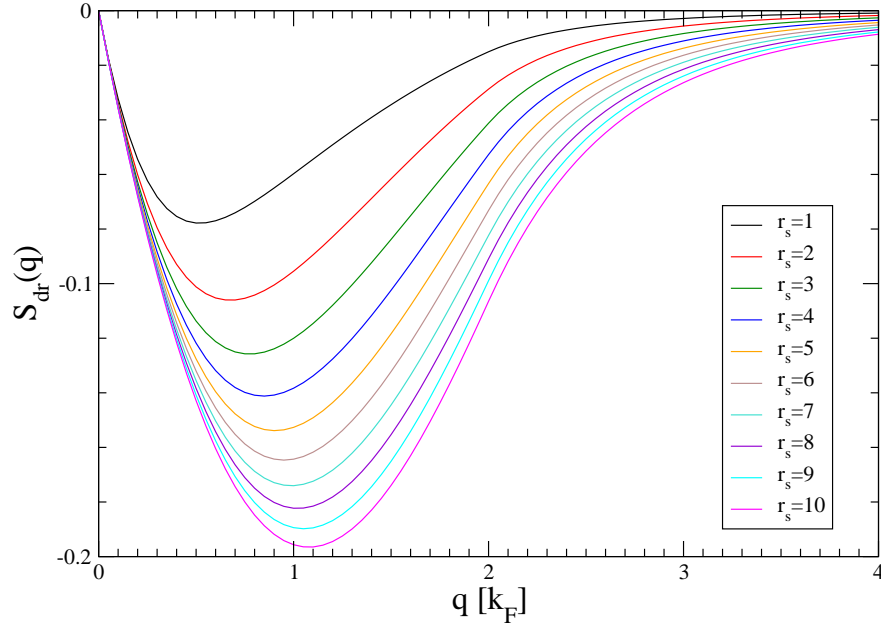


FIG. 4: Direct structure factor in RPA according to Eq. (15), evaluating the diagram in Fig. 1(c).

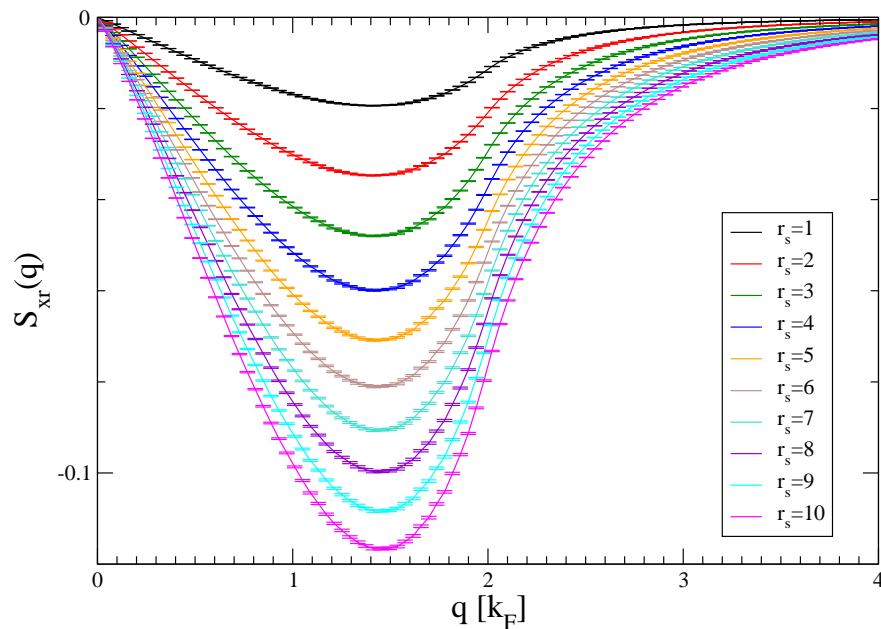


FIG. 5: Second order exchange structure factor in RPA according to Eq. (18), evaluating the diagram in Fig. 2(c). The error bars show the 95% confidence interval of the MC integration.